Catal Lett (2010) 138:68–75
DOI 10.1007/s10562-010-0370-8

Selective Liquid-phase Hydrodechlorination of Chlorotrifluoroethylene over Palladium-Supported Catalysts: Activity and Deactivation

Bao-Chuan Meng · Zhao-Yang Sun · Jin-Peng Ma · Gui-Ping Cao · Wei-Kang Yuan

Received: 8 December 2009 / Accepted: 10 May 2010 / Published online: 22 May 2010

Abstract Liquid-phase hydrodechlorination of chlorotrifluoroethylene (CTFE) to trifluoroethylene (TrFE) with molecular hydrogen was studied over palladium-supported catalysts. $BaSO_4$, Al_2O_3 and activated carbon (AC) were used as supports, respectively. The results showed that the Pd/AC catalysts exhibit higher activity than Pd/$BaSO_4$ and Pd/Al_2O_3. The treatment of activated carbon with HNO_3 led to a considerable increase of surface functional groups containing oxygen atoms, which resulted in a higher dispersion of palladium on the supports and enhancement of catalytic activity. The stability of the catalyst was investigated, one reason for the inhibition was the accumulation of NaCl on the surface of Pd/AC that blocks the pores of carbon support. The activity of Pd/AC could partially recovered by washing with water. The other irreversible deactivation of the catalyst are from the change of particle size and the pore structure, leaching of Pd, a decrease of BET surface area and Pd surface area of Pd/AC catalyst.

Keywords Trifluoroethylene · Activated carbon · Pd/AC catalyst · HNO_3 pretreatment · Deactivation

1 Introduction

Chlorinated organic compounds exhibit high toxicity and form a class of environmentally undesirable compounds that are produced by a wide range of industrial processes as by-products [1]. Catalytic hydrodechlorination of chlorinated organic compounds over noble metal catalysts has been recognized as a facile and efficient procedure to eliminate these compounds [2, 3]. Among noble metals in Group VIII known for those procedures, palladium was reported to be the most active metal that catalyze selective replacing of chlorine with hydrogen. As Pd not only promotes C–Cl bond cleavage efficiently, but also shows poisoning resistance [4, 5].

Heterogeneous catalytic hydrodechlorination is conventionally carried out in either gas [6–8] or liquid phase [2, 3, 9]. The hydrogen source can be molecular hydrogen [3, 6, 10] or other hydrogen donors such as alcohols, 2-propanol [11, 12], sodium hypophosphite, sodium borohydride [13], as well as proaromatic compounds [14].

Trifluoroethylene (TrFE), produced by catalytic hydrodechlorination of chlorotrifluoroethylene (CTFE), is an important chemical intermediate for synthesis of many useful compounds. For example, 1,1,1,2-tetrafluoroethane (HFC-134a) is known as the best alternative of freons. It also can copolymerize with olefins, for instance, the copolymerization product of TrFE with vinylidene fluoride (VDF) has extraordinarily piezoelectric and pyroehctric properties, that are widely used as transducers or detectors [15].

Porosity and surface area of the catalyst support have remarkable effects on the catalytic activity and selectivity. Francisco R R [16] found that in many cases the catalyst properties were a function of porosity and surface area, which was relatively straightforward, as the microporosity is responsible for the high surface area of activated carbons act as support to the deposited metal particles, thus favoring large dispersion. Activated carbon with high surface area and a well controlled porosity is essential to metal dispersions, which usually results in a high catalytic activity and selectivity. It was also found that the properties

---

B.-C. Meng · Z.-Y. Sun · J.-P. Ma · G.-P. Cao (✉) · W.-K. Yuan
East China University of Science and Technology, UNILAB Research Center of Reaction Engineering, State-key Laboratory of Chemical Engineering, Shanghai 200237, China
e-mail: gpcao@ecust.edu.cn

of activated carbon were determined by not only its surface area and pore structure, but also the amount of surface functional groups [16, 17]. After pretreated with strong oxidizing agents, such as HNO_3 or H_2O_2, more oxygen containing functional groups such as –OH and –COOH are created on the surface of activated carbon [16], which would enhance the interaction of the surface sites with guest molecules. Surface treatment makes the carbon surface more hydrophilic and accessible to the aqueous solution of metal precursors during impregnation.

Unfortunately, major drawback of the hydrodechlorination catalyst is its deactivation. Catalyst stability is recognized as very important aspect of catalyst studies for industry and academia [18]. Thereby, since it is crucial to optimize processing conditions and avoid premature catalyst deactivation. Yet, researches on catalyst deactivation receive less attention than the discovery of new catalysts [18].

Urbano and Marinas [14] have reported that the deactivation of the catalysts has been related to several factors, i.e. the inhibitory effect of HX formed as by-product, formation of carbonaceous deposits, sintering of the active phase and degradation of the catalyst by the corrosive acid formed in the reaction. However, formation of carbonaceous and sintering of the active metal are common specially in the gas phase hydrodechlorination processes [8, 19] rather than liquid phase. At present, it is widely accepted that the HCl formed from the hydrodechlorination reaction is the main reason to inhibit the activity of palladium metal-supported catalysts. This inhibition effect of the reaction product HCl, is manifested in a negative reaction order (-1), as reported by Somorjai and co-workers [20, 21] working with model catalysts.

The negative effect of HCl may result from two essential factors. Firstly, the competitive adsorption between HCl and the substrate on the palladium surfaces as reported by Coq [4], in his study on gas-phase hydrogenolysis of chlorobenzene. Secondly, the corrosive medium produced from the acid released may degrade either the support [9] or the metal phase [22] of the catalyst. That is the reason why a base, such as $H_2N–R–NH_2$, Zn powder, NaOH, KOH, etc. is normally added to neutralize HCl and avoid catalyst deactivation [2, 3, 10, 14].

Furthermore, the catalysts degradation due to the corrosive environment in the reaction system also should be taken into account, e.g. Forni et al. [23] detected 25% of the BET area and 20% of palladium leaching from the catalyst after running for 20 h in the process of hydrodechlorination of Polychlorinated biphenyls (PCBs) on Pd/C. Similar results were corroborated by Concibido et al. [3] and Cobo et al. [11].

However, for the hydrodechlorination of CTFE to TrFE over palladium-supported catalysts, little information is available in literature including the type of catalyst, the processing conditions and catalyst deactivation.

In this paper, different catalyst supports such as $BaSO_4$, Al_2O_3 and activated carbon were used to load palladium. Bohem titration for determining surface groups, N_2 physical adsorption and Scanning Electron Microscope (SEM) were adopted to examine the changes of physical and chemical properties of the surface of activated carbon after treated with HNO_3, respectively. CO chemisorption and Transmission Electron Microscopy (TEM) were conducted to clarify the effect of activated carbon pretreatment on the dispersion of Palladium. In addition, we compared the activity and selectivity of the Pd/AC catalysts whose supports that were treated with and without HNO_3, respectively. Furthermore, the stability of the Pd/AC catalyst was evaluated, and the deactivation mechanism was discussed on the basis of the characterization of fresh and used catalysts.

2 Experimental

2.1 Materials

Chlorotrifluoroethylene (purity = 99.5%) was obtained from Shanghai 3F New Materials CO., Ltd., and used without further purification. $PdCl_2$ and all other chemical reagents (minimum 96% purity) used in the experiments were purchased from Sinopharm Chemical Reagent Co., Ltd. The activated carbon having a BET surface area of 1397 m^2/g, and a mean particle size of about 50 μm was purchased from SHHXTC. Ultrapure water (Advantec RFD25ORA Water Distilling Apparatus) was used in all the experiments. Hydrogen and nitrogen with the purities of 99.99% were purchased from Shanghai Jifu Gas Co., Ltd.

2.2 Pretreatment of Activated Carbon and Characterization

The typical procedure of pretreatment of activated carbon was as follows: 10 g of activated carbon original was introduced in 100 mL HNO_3 (10 wt%) solution and stirred at 90 °C under reflux for 4 h to ensure that the volume was kept constant along the process. After the treatment, samples were washed with ultrapure water until neutral pH and dried in oven at 110 °C overnight. This sample was labeled as AC1. The activated carbon without treated by HNO_3 was washed with ultrapure water until neutral, and noted as AC0.

Bohem titration with different strength of bases was used to determine the contents of various functional groups containing oxygen atoms on the surface of activated carbon (AC0 and AC1), bases where NaOH was used for determining the amount of carboxyl groups, Na_2CO_3 for that of lactones and carboxyl groups, NaOH for that of phenols, lactones and carboxyls and $NaOC_2H_5$ for that of carbonyl, phenols, lactones and carboxyls, respectively [24, 25]. Weighed amount of activated carbon sample (about 1.0 g) was placed in 25 mL of 0.1 M solution of the base. After sealing and equilibration with gentle agitation for 48 h at 30 °C, then the suspension was filtered. 10 mL of the filtrate was pipetted and 50 mL standard 0.1 M HCl solution was added to it, back-titrated with standard 0.1 M NaOH. The content of all those functional groups containing oxygen atoms were calculated according to the assumption of NaOH solution neutralizing acidic groups.

The amounts of alkali consumption during these procedures can be given by Eq. 1.

$$b = (V \times c_{\mathrm{NaOH}} + 25 \times c_0 - 50 \times c_{\mathrm{HCl}})/m \tag{1}$$

where b is the amount of alkali consumption (mmol/g), V is the volume of sodium hydroxide solution which used to titrate excessive HCl (mL), c_0 is the concentration of base used (mol/L), and m is the amount of activated carbon samples (g).

So, the content of carboxyl groups, lactone groups, phenolic groups, carbonyl groups, acidic surface function groups can be expressed as $b_{\mathrm{NaHCO_3}}$, $b_{\mathrm{Na_2CO_3}}$–$b_{\mathrm{NaHCO_3}}$, b_{NaOH}–$b_{\mathrm{Na_2CO_3}}$, $b_{\mathrm{NaOC_2H_5}}$–b_{NaOH}, and $b_{\mathrm{NaOC_2H_5}}$ (mmol/g), respectively.

2.3 Catalyst Preparation and Characterization

Pd/AC, $Pd/BaSO_4$ and Pd/Al_2O_3 catalysts were prepared by wet impregnation method. The precursor used was $PdCl_2$ and the supports were impregnated with aqueous solution of the precursor in the appropriate concentration. After the impregnation procedure, the mixture was filtered. Then, the catalysts were dried at 110 °C overnight and followed by calcination in nitrogen stream at 400 °C for 4 h. Finally, the catalysts thus obtained were reduced in hydrogen stream at 300 °C for 4 h. Pd content of those catalysts was 3 wt%.

The nitrogen adsorption–desorption isotherms were measured on a Micromeritics ASAP 2010 analyzer (USA). The samples were degassed at 190 °C for 6 h to remove the surface impurities. The surface area was determined by adsorption of nitrogen at 77 K and calculated using the Brunauer–Emmett–Teller (BET) method. The pore size distributions were calculated using the Barrett–Joymer–Halenda (BJH) method on the adsorption branch.

Scaning electron microscopy (SEM) was employed to get insight into the morphology of the samples. Samples were sputtered with gold and the images were acquired in JEOL JSM6360LV (Japan) operated at 20 kV.

Transmission electron microscopy (TEM) images were collected using a JEOL JEM 2100 (Japan) electron microscope with a LaB_6 filament as the source of electrons, operating at 200 kV.

Pd dispersion and average active particle size of the catalyst was determined by measuring CO pulse-adsorption (Micromeritics Autochem 2910) in a flow of helium after reduction in 10% H_2–N_2 at 450 °C for 2 h. The catalyst surface was cleaned by heating in a flow of helium at 120 °C for 1 h. The palladium dispersion was calculated with respect to the total carbon monoxide uptake by assuming that carbon monoxide was adsorbed on surface palladium atoms at a stoichiometric ratio of 1:1.

The powder catalyst particle size distribution was evaluated by laser diffraction using a Mastersizer 2000 analyzer (Malvern Instrument).

Atomic absorption spectrometry (AAS) was used to determination the Pd content of the catalyst samples. The procedure is as follows: aqua regia was added to a known amount of the catalyst and the mixture was evaporated to dryness. The final residue was then dissolved in 0.1 mol/L HCl to a volume of 50 mL [3] and the solution was analyzed using TJA IRIS 1000.

2.4 Hydrodechlorination Procedure

The liquid-phase hydrodechlorination of CTFE with molecular hydrogen was carried out in a 1-L high pressure bath reactor. Gauges were equipped to record the pressure and temperature inside the reactor throughout the experiment.

A typical operational procedure used in each experiment was as follows: a certain amount of CTFE, methanol, water, sodium hydroxide and catalyst samples were added in the reactor respectively. After the temperature leveled off at 100 °C, which spent about 30 min, the reactor was charged with hydrogen to the pressure of 1.25 MPa. Simultaneous, the stirring device started and the reaction timed. In the end of the experiment, the reactor was cooled to room temperature and the products were collected and analyzed by a gas chromatograph equipped with a flame ionization detector (FID). All products were identified by Micromass GCTTM GC-mass spectroscopy. The main product was TrFE, in addition, a small amount of vinylidene fluoride (VDF) was detected.

The reaction equation is:

$$CF_2 = CFCl + H_2 \rightarrow CF_2 = CHF + HCl$$

In addition to the main reaction, there is a follow-up reaction as follows to produce by-product,

$$CF_2 = CHF + H_2 \rightarrow CH_2 = CF_2 + HF$$

The conversion of CTFE and selectivity of TrFE were calculated using Eqs. 2 and 3.

$$\text{conversion}_{\text{CTFE}} = \frac{\text{Feed CTFE (mol)} - \text{Unreacted CTFE (mol)}}{\text{Feed CTFE (mol)}} \times 100(\%) \tag{2}$$

$$\text{selectivity}_{\text{TrFE}} = \frac{\text{TrFE produced (mol)}}{\text{Feed CTFE (mol)} - \text{Unreacted CTFE (mol)}} \times 100(\%) \tag{3}$$

3 Results and Discussions

3.1 The Effect of Different Catalyst Support

The activities of the synthesized catalysts were investigated in the hydrodechlorination of CTFE to TrFE in a batch autoclave and the experimental results were displayed in Fig. 1. It is seen from Fig. 1 that Pd/AC1 is the most active catalyst, followed by Pd/AC0, Pd/Al_2O_3 and Pd/$BaSO_4$, i.e. activated carbon is superior to Al_2O_3 and $BaSO_4$ when used as catalyst support, and the N_2 physisorption data of the catalysts are shown in Table 1. Table 1 shows that this phenomenon can attributed to high surface area and well developed porosity of activated carbon which are essential for achieving large metal dispersions and high catalytic activity. It also can be seen from Fig. 1 that Pd/AC1 appears higher catalytic activity compared to Pd/AC0, whose reason will be interpreted in Sect. 3.3.

3.2 Blank Experiments with CTFE

In order to find out whether any reaction product can be formed in the absence of palladium-supported catalyst, several experiments with hydrogen and CTFE were made under the same conditions as the catalytic reaction, namely: (i) using activated carbon original (AC0) as “catalyst”; (ii) using activated carbon after treatment with HNO_3 (AC1) as “catalyst”; (iii) without any solid. In these three cases, the conversion of CTFE was not detected.

3.3 The Effect of HNO_3 Pretreatment on Activated Carbon

The influence of HNO_3 treatment on textural properties and apparent morphology of activated carbon (AC0 and AC1) is shown in Table 1 and Fig. 2, respectively. It is demonstrated in Table 1 and Fig. 2 that HNO_3 pretreatment has no significant impact on textural properties though BET surface area of AC1 decreased slightly and apparent morphology was changed little. It is generally reported that the liquid phase oxidation does not change the texture of activated carbons significantly [27, 28], although under more drastic conditions a decrease in surface area and pore volume has been observed while the average micropore width increases, as a result of the collapse of pore walls [29].

The contents of functional groups containing oxygen atoms on AC0 and AC1 were analyzed by Bohem titration method, and the results are shown in Table 2. As shown in Table 2, although the concentration of lactone groups decreases slightly, the activated carbon treated with HNO_3 obviously possesses higher concentration of functional groups containing oxygen atoms, in which carboxyl groups increase significantly. This can be interpreted from the mechanism for carbon oxidation proposed by Figueiredo et al. [27] as follows.

$$C_f + O_2 \rightarrow \text{carbonyls, ethers}(+CO) \tag{I}$$

$$C_f + O_2 \rightarrow \text{lactones, anhydrides} \tag{II}$$

$$C_f + \text{carbonyls, ethers} + O_2 \rightarrow CO_2 + CO \text{ or carbonyls, ethers} \tag{III}$$

$$C_f + \text{carbonyls, ethers} + O_2 \rightarrow \text{lactones, anhydries} \tag{IV}$$

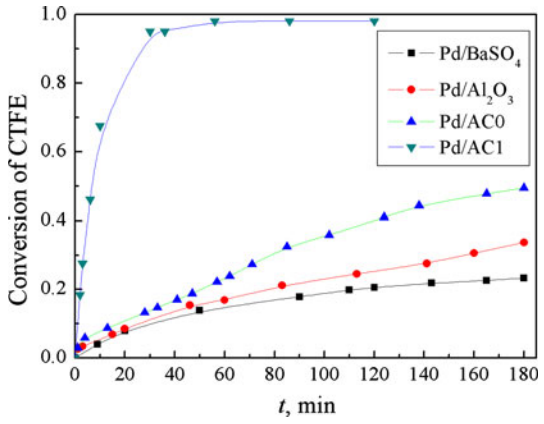

Fig. 1 The results on different catalysts

Table 1 The N_2 physisorption data of different catalysts, activated carbon treated with and without HNO_3, respectively, and the catalyst after 10 runs

Catalyst	BET surface area, m^2/g	Pore volume, cm^3/g	Pore size, nm
Fresh Pd/$BaSO_4$	7.13	0.010	20.810
Fresh Pd/Al_2O_3	136.74	0.230	4.950
AC0	1397.34	0.390	2.180
Fresh Pd/AC0	1411.25	0.350	2.170
AC1	1175.29	0.330	2.170
Fresh Pd/AC1	1188.20	0.300	2.160
Pd/AC1 after 10 runs	373.32	0.077	2.350

AC0 the activated carbon without the treatment of HNO_3, *AC1* the activated carbon with the treatment of HNO_3

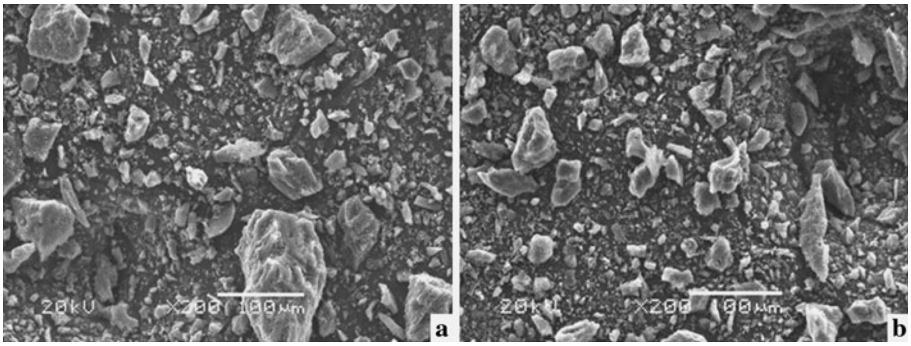

Fig. 2 SEM images of AC0 (**a**) and AC1 (**b**)

Table 2 The concentration s of functional groups containing oxygen atoms in AC0 and AC1

Activated carbon	Carboxyl groups, mmol/g	Lactone groups, mmol/g	Phenolic hydroxyl groups, mmol/g	Carbonyl groups, mmol/g	Acidic surface function groups, mmol/g
AC0	1.0064	0.0803	0.2749	0.6118	1.9734
AC1	1.7700	0.0605	0.4104	0.8730	3.1140

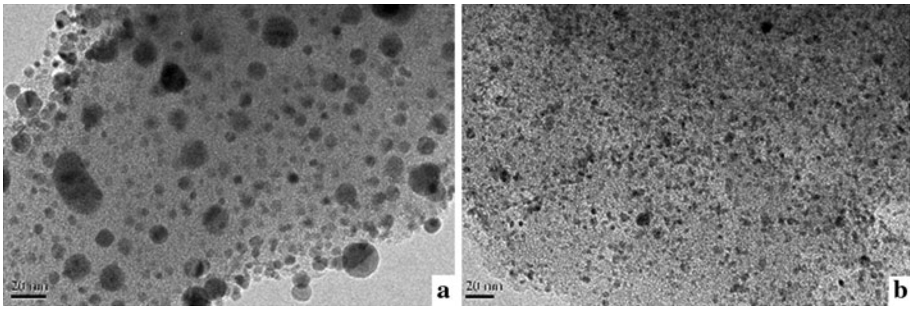

Fig. 3 TEM images of Pd/AC0 (**a**) and Pd/AC1 (**b**)

$$\text{lactones, anhydries} \rightarrow CO_2(+\ CO) +\ 2C_f \qquad (V)$$

$$\text{carbonyls, ethers} \rightarrow CO + C_f \qquad (VI)$$

where, C_f is a free active site on the activated carbon surface. Reactions (V) and (VI) related to the decomposition of the surface groups can be neglected. It was reported that the gas phase oxidation of activated carbon mainly increases the concentration of hydroxyl and carbonyl surface groups, while oxidation in the liquid phase increases especially the concentration of carboxylic groups [27].

As shown above, activated carbon treated with HNO_3 produced a decrease in surface area and microporosity due to the destruction of the pore walls by the oxidation treatment. The concentration of functional groups containing oxygen atoms increased significantly especially for carboxylic groups, which made the surface more accessible to the aqueous solutions of the metal precursors during impregnation. It is reported [16] that in impregnation step, the interaction of palladium precursor with activated carbon is favored by the presence of oxygen surface groups, which make the carbon surface more hydrophilic, and thus, a better dispersion of the palladium precursor is achieved.

To clarify the effect of activated carbon pretreatment on the dispersion of palladium, TEM and CO chemisorption were conducted with Pd/AC catalysts respectively and TEM images of Pd/AC0 and Pd/AC1 were present in Fig. 3. As is seen in Fig. 3, when HNO_3 treated activated carbon (AC1) is used as support, the catalyst gave a quite smaller size of Pd particles and a quite higher dispersion of Pd particles. We selected randomly about 50 Pd particles from Fig. 3a and b, respectively, measured the diameters of the particles, and calculated the average diameters. The average Pd particles diameter is 11.984 nm on Pd/AC0, and 4.923 nm on Pd/AC1.

Table 3 presents the dispersion and the average particle size of Palladium catalysts on the activated carbon determined by CO chemisorption. The diameter of Pd particles is 14.1856 nm on Pd/AC0, and 5.3518 nm on Pd/AC1, which are agree well with that from TEM images. Obviously, it can be seen from Table 3 that Pd dispersion Pd/AC1 is significantly improved compared to Pd/AC0, and the particle size of palladium is smaller. The results of Fig. 3 and Table 3 show that Pd dispersion of a carbon-supported Pd catalyst is closely related to the concentration

Table 3 CO chemisorption results of Pd/AC0, Pd/AC1 fresh and after used 10 runs

Catalyst	Pd dispersion, %	Pd particle diameter, nm	Pd surface area, m^2/g metal
Fresh Pd/AC0	7.8986	14.1856	35.1883
Fresh Pd/AC1	20.9363	5.3518	93.2710
Pd/AC1 after 10 runs	18.2974	6.1237	81.5148

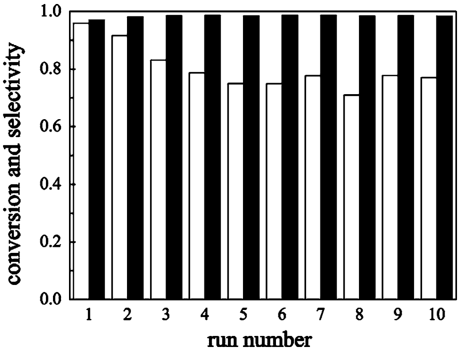

Fig. 4 Activity and selectivity of Pd/AC1 catalyst used in repeated hydrodechlorination runs (*open square*—conversion of CTFE; *filled square*—selectivity of TrFE)

of functional groups containing oxygen atoms on activated carbon which make the carbon surface more hydrophilic and a high Pd dispersion was achieved.

3.4 The Lifespan of Pd/AC1 Catalyst

The Pd/AC1 catalyst was recovered after each run and directly reused in the next run using a fresh solvent. Moreover, NaOH was added to eliminate HCl liberated in the hydrodechlorination reaction. Ten hydrodechlorination runs with the same catalyst were carried out in the mixture of methanol and water. The result of lifespan test of Pd/AC1 catalyst is shown in Fig. 4. As shown in Fig. 4, the activity of Pd/AC1 catalyst decreased slightly in the first three runs, and then maintained stability up to the 10th run. For the first run, the fresh catalyst was used, and the conversion of CTFE is 95.96%. However, after the 10 runs of the catalyst, the conversion of CTFE decrease to 77.04%. There is about 19.72% of activity of the catalyst was lost. Meanwhile, the selectivity of TrFE after the first cycle remained unchanged (>97%). The dissociation energies of C–F and C–Cl bonds are 109 and 81 kcal/mol, respectively [29]. Due to the more strength of the C–F bond, fluorides are more resistant to the hydrogenation. This difference makes it possible for the selective hydrodehalogenation reactions in polyhalides containing different halogen atoms [10]. For hydrodehalogenation of CTFE, the main product is TrFE favorable while the quantity of VDF can be ignored.

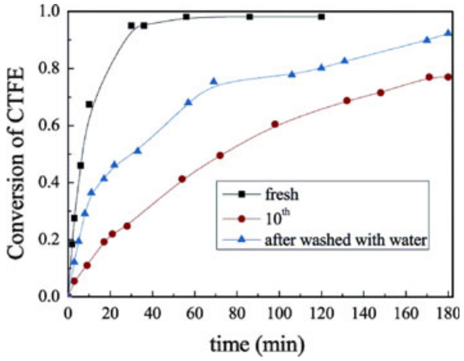

Fig. 5 Reactivation of Pd/AC1 catalyst with water after 10 runs

3.5 Recovering the Used Catalyst by Aqueous Washing

Washing the used catalyst desorbs the substance that adsorbed on the surface of the catalyst. This method is facile to identify the causes of the catalyst deactivation; moreover, the reactivated catalyst could be regenerated. Thus, the catalyst used after 10 runs was recovered and washed by stirring in water for 24 h, before a new hydrodechlorination run using a fresh solvent was carried out.

Figure 5 shows that washing the catalyst with water could recover the catalytic activity partially, which signified that it is effective in washing out the substances absorbed on the catalyst.

It has been reported that in the catalytic hydrodehalogenation reaction, the addition of bases, e.g. NaOH or NH_3, is effective in suppressing the deactivation of catalyst, because the halogen ions responsible for the poisoning are removed from the catalyst surface [3, 14]. Salts produced in the reactions such as NaCl are likely to deposit on the catalyst surface decreasing the catalytic activity; washing the catalyst with water could restore the activity of the catalyst [3, 10, 30]. Ukisu et al. [31] in their studies on hydrogenation of aromatic chlorides over Rh-Pt/C catalyst have found that the activity of the catalyst gradually decreased attribute to the accumulation of NaCl on the catalyst surface and water could wash away these salts and the activity of the catalyst could recovered completely.

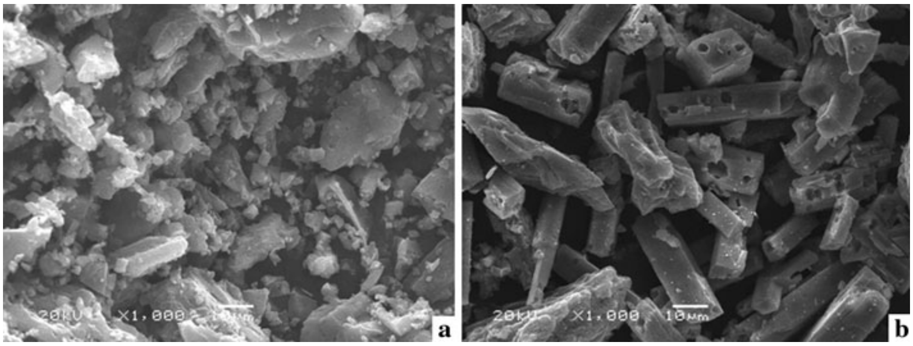

Fig. 6 SEM images of Pd/AC1 catalysts fresh (**a**) and after used 10 runs (**b**), respectively

3.6 Other Factors for Deactivation

In Sect. 3.5, we found that NaCl accumulation on catalyst surface is one of the reasons causing deactivation, and after washed with water, the catalytic activity could recover partially, so there must be other reasons causing deactivation.

The SEM images of Pd/AC1 catalysts fresh and after used for 10 runs are shown in Fig. 6. It is clearly observed from Fig. 6 that the particle size and pore structure of the catalyst are changed, i.e. catalyst reuse procedure decreased the porosity and BET surface area of the activated carbon, the results of Nitrogen adsorption–desorption analysis shows that the BET surface area, pore volume and pore size are decreased from 1188.20 m^2/g, 0.30 cm^3/g, 2.16 nm to 373.32 m^2/g, 0.077 cm^3/g, 2.35 nm respectively after used 10 runs (see Table 1). Support pore occlusion and partial destruction of the support structure have been recognized as possible reasons for surface area decrease [32].

The particle size distribution of Pd/AC1 catalysts (fresh and after 10 runs) was also characterized, and the results are shown in Table 1 and Fig. 7. The results from Table 1 and Fig. 7 strengthened the conclusion shown in Fig. 6 that the particle size distribution of Pd/AC1 after 10 runs was more non-uniform, i.e. the number of small particle decreased slightly while the number of big particle increased significantly, which also leads to a decrease of BET surface area and catalytic activity.

According to the results of CO chmisorption shown in Table 3, Pd/AC1 after 10 runs showed a slightly decrease in Pd disperision and Pd surface area, and at the same time, particle size of Pd increased a bit.

In order to determine the difference between the fresh and the used catalyst, the palladium content of the catalyst after 10 runs was also detected via AAS method. The Pa content of the catalyst after 10 runs is 2.394%. Compared with that of the fresh catalyst (3% Pd), there were about 20.2% of Pd lost from the catalyst after used 10 runs, which agrees well with the results shown in Fig. 4. The main reason of deactivation of the catalyst was Pd losing from the catalyst, which also contribute to the inreversible deactivation of catalyst.

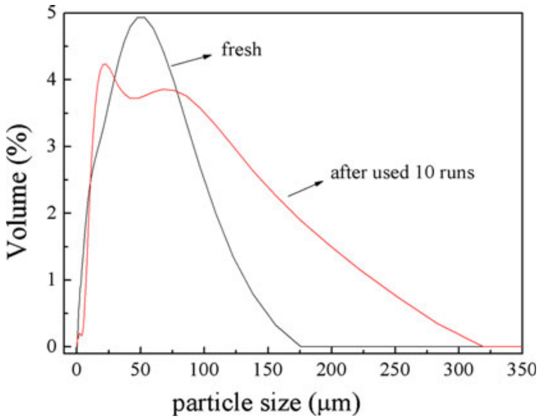

Fig. 7 The particle size distribution of Pd/AC1 catalyst fresh and after used 10 runs

4 Conclusions

The results obtained in the catalytic hydrodechlorination of CTFE over various palladium-supported catalysts allow us to draw several interesting conclusions as regards effects of supports of the catalyst and the reasons of catalyst deactivation.

(1) Because of high surface area and well developed porosity of activated carbon, Pd/AC catalysts show higher activity than Pd/Al_2O_3 and Pd/$BaSO_4$.

(2) Activated carbon after HNO_3 treatment produced a decrease in surface area and microporosity due to the destruction of the pore walls by the oxidation treatment. While the concentration of functional groups containing oxygen atoms was increased significantly especially carboxylic groups, which make the carbon surface more hydrophilic, and thus, a better dispersion of the palladium precursor is achieved.

(3) The stability of Pd/AC1 catalyst was investigated. The catalyst exhibits a slightly deactivation in

repeated runs while the used catalyst after washed with water, the activity could recovered partially, signifying that the reversible deactivation was due to the accumulation of NaCl on the surface of Pd/AC and blocks the pores of carbon support and washing with water could remove it.

(4) The irreversible deactivation of the Pd/AC1 catalyst attributed to the change of particle size and the pore structure, losing of palladium, decrease of BET surface area and Pd surface area.

Acknowledgements This work is financially supported by Shanghai 3F New Materials CO., Ltd. and Shanghai Huayi (Group) Company.

References

1. Murena F, Famiglietti V, Gioia F (1993) Environ Prog 12:231
2. Aramendia MA, Borau V, Garcia IM et al (2002) J Mol Catal A: Chem 184:237
3. Concibido NC, Okuda T, Nishijima W et al (2007) Appl Catal B 71:64
4. Coq B, Ferrat G, Figueras F (1986) J Catal 101:434
5. Kulkarni PP, Deshmukh SS, Kovalchuk VI et al (1999) Catal Lett 61:161
6. Srinivas ST, Jhansi Lakshmi L, Lingaiah N et al (1996) Appl Catal A 135:201
7. Barrabes N, Cornado D, Foettinger K et al (2009) J Catal 263:239
8. Meshesha BT, Chiment RJ, Medina OF et al (2009) Appl Catal B 87:70
9. Aramendia MA, Borau V, Garcia IM et al (1999) J Catal 20:392
10. Xia C, Xu J, Wu W et al (2004) Catal Commun 5:383
11. Cobo M, Quintero A, Correa CMD (2008) Catal Today 133–135:509
12. Ukisu Y (2008) Appl Catal A 349:229
13. Pri-Bar I, James BR (2007) J Mol Catal A: Chem 264:135
14. Urbano FJ, Marinas JM (2001) J Mol Catal A: Chem 173:329
15. Pinto NJ, Bao ZX (1998) Chin J High Press Phys 12:223
16. Rodriguez-Reinoso F (1998) Carbon 36:159
17. Pigamo A, Besson M, Blanc B et al (2002) Carbon 40:1267
18. Birtill JJ (2003) Catal Today 81:531
19. Wiersma A, van de Sandt E, den Hollander MA et al (1998) J Catal 177:29
20. Rupprechter G, Somorjai GA (1997) Catal Lett 48:17
21. Ribeiro FH, Gerken CA, Somorjai GA et al (1997) Catal Lett 45:149
22. Hoke JB, Gramiccioni GA, Balko EN (1992) Appl Catal B 1:285
23. Forni P, Prati L, Rossi M (1997) Appl Catal B 14:49
24. Boehm HP (1994) Carbon 32:759
25. Boehm HP (2002) Carbon 40:145
26. Alonso F, Beletskaya IP, Yus M (2002) Chem Rev 102:4009
27. Figueiredo JL, Pereira MFR, Freitas MMA et al (1999) Carbon 37:1379
28. Noh JS, Schwarz JA (1990) Carbon 28:675
29. Moreno-castilla C, Carrasco-marin F, Maldonado-hodar FJ et al (1998) Carbon 36:145
30. Xia C, Liu Y, Xu J et al (2009) Catal Commun 10:456
31. Ukisu Y, Kameoka S, Miyadera T (2000) Appl Catal B 27:97
32. Yuan G, Keane MA (2003) Catal Today 88:27